

Optical Properties of Cholesteric Liquid Crystals

R. Dreher and G. Meier

*Institut fuer Angewandte Festkoerperphysik der Fraunhofer-Gesellschaft, Eckerstrasse 4,
D-7800 Freiburg i. Br., Germany*

(Received 5 March 1973; revised manuscript received 22 May 1973)

A general theory of wave propagation in helical structures is developed. It is shown that this problem is quite similar to the well-known wave propagation in solid crystal lattices. If energy dissipation is neglected there are shown to exist frequency bands for wave propagation without attenuation separated by frequency bands where waves are damped out and cannot propagate. Formally, the waves have the form of Bloch waves $e^{i\vec{k}\cdot\vec{r}}u(\vec{r})$, having the character of plane waves modulated by a function $u(\vec{r})$ which is periodic with the structure. Based on this theory, for reflection of light by homogeneously ordered cholesteric liquid crystals the following results are obtained: For incident light parallel to the helical axis there exists only one band of selective reflection. For obliquely incident light, however, an infinite series of higher-order reflection bands occur. Each reflection band is split into two branches. The angular dependence of the reflection bands and the sequence of the higher-order reflections on the wavelength scale bear a certain analogy to Bragg reflection.

INTRODUCTION

In this paper, light-wave propagation in helicoidal structures is theoretically investigated with the special aim to interpret the selective reflection of light by cholesteric liquid crystals caused by the screwlike or helicoidal arrangement of their molecules. The results, however, are quite general and may also be applied to completely different systems.

A helicoidal structure is primarily a periodic structure. Therefore one would expect that the wave propagation in this type of structure would be similar to that in solid crystal lattices. In solid crystals, however, the structural periodicity is of the order of magnitude of Å units, whereas in cholesteric liquid crystals the pitch of the helix generally has values between 1000 Å and infinity. If one adopts the simple model of Bragg reflection for the helicoidal liquid crystal, then one should expect a selective reflection of light to occur in the visible region and for longer wavelengths rather than in the x-ray region. This visible reflection actually does occur and it is a well-known feature of cholesteric liquid crystals. In fact, Bragg's law has been used in attempts to explain the wavelength and angular dependence of this selective reflection in cholesteric liquid crystals.¹ The model of a Bragg reflection, however, is far too simple and does not explain the lack of higher-order reflections at normal incidence and the width of the reflection bands.

Rigorous theoretical treatments of the problem for light propagating parallel to the helix were made first by Oseen² and later by de Vries.³ In addition, Oseen considered the more complicated general case of light propagating obliquely to the

helix. More recently, Berreman and Scheffer⁴ and Taupin⁵ treated this case by numerical procedures using the method of propagation matrices.

In this paper, a more complete analytical approach is developed which treats the wave propagation in a helicoidal medium for arbitrary wave vectors and which results in a diagram similar to a zone scheme first introduced by Brillouin for solid crystals. This diagram, referred to as the "chart of stability" will indicate the conditions for which the structure acts as bandpass (transmission) or bandstop (reflection) filter. It is the fundamental result of this work. This chart of stability reveals many details concerning the wave propagation, but gives no information about the intensities of the waves.

WAVE EQUATION AND SOLUTIONS

We are considering a cholesteric liquid crystal with a uniformly twisted structure. It is described macroscopically by its dielectric tensor. Energy dissipation by absorption is neglected. Assuming the liquid crystal to be locally uniaxial we adopt that the axis \vec{L} of the dielectric tensor ellipsoid is directed perpendicular to the helical axis at any point. If the screw axis is taken to be parallel to the z axis of a space-fixed coordinate system x, y, z , \vec{L} varies continuously with z :

$$\vec{L} = \{\cos\alpha, \sin\alpha, 0\}; \quad \alpha = (2\pi/p)z. \quad (1)$$

Here we have introduced the pitch p that is the distance for a complete turn of the local optical axis.

The dielectric tensor $\|\epsilon\|$ of the cholesteric liquid crystal which relates the electric field \vec{E} to the dielectric displacement vector \vec{D} ,

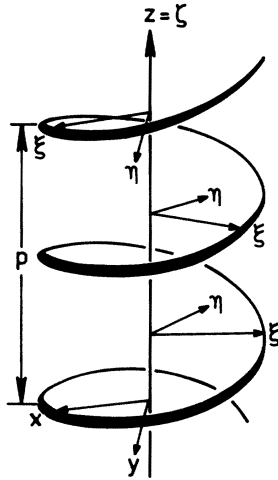


FIG. 1. Definition of coordinate systems. In a space fixed coordinate system (x, y, z) the local optical axis \vec{L} of a cholesteric liquid crystal describes a helix. A variable coordinate system (ξ, η, ζ) may be chosen so that the dielectric tensor is diagonal therein.

$$\vec{D} = \|\epsilon(\alpha)\| \cdot \vec{E}, \quad (2)$$

is a function of the twist angle $\alpha = (2\pi/p)z$. It can be written in the laboratory coordinate system (x, y, z) (see Fig. 1) as

$$\begin{pmatrix} \epsilon(1 + \beta \cos 2\alpha) & \epsilon\beta \sin 2\alpha & 0 \\ \epsilon\beta \sin 2\alpha & \epsilon(1 - \beta \cos 2\alpha) & 0 \\ 0 & 0 & \epsilon_3 \end{pmatrix}. \quad (3)$$

Here we have introduced an average dielectric constant $\epsilon = \frac{1}{2}(\epsilon_1 + \epsilon_2)$ and a dielectric anisotropy $\beta = (\epsilon_1 - \epsilon_2)/(\epsilon_1 + \epsilon_2)$.

It is convenient to define also a local Cartesian coordinate system (ξ, η, ζ) with $\xi \parallel \vec{L}$ and $\zeta \parallel z$. In this local coordinate system the dielectric tensor is in a diagonal form having the principle values

$$\epsilon_1 = \epsilon(1 + \beta), \quad \epsilon_2 = \epsilon(1 - \beta), \quad \epsilon_3. \quad (4)$$

In order to study wave propagation in the twisted structure we have to solve Maxwell's equations or the equivalent wave equation given by

$$\frac{1}{c^2} \frac{\partial^2 \vec{D}}{\partial t^2} = \Delta \vec{E} - \text{grad div} \vec{E}. \quad (5)$$

Here the magnetic susceptibility is neglected. \vec{D} and \vec{E} are connected by (2). In the first step of our calculations we assume that there is an electromagnetic field in the material. It can be produced, e.g., by light incident to a boundary which is normal to the twist axis. We seek waves that will not propagate in the structure. This gives the reflection bands. In a second step we will then introduce the boundary explicitly.

Like in other periodic structures, waves in a twisted material are generally not simple plane waves. We therefore try solutions that have only the plane wave form for the dependence on the direction normal to the helical axis—say, the x axis—but with arbitrary dependence in the z direction:

$$\begin{bmatrix} E_x \\ E_y \\ E_z \end{bmatrix} = \begin{bmatrix} F_1(z) \\ F_2(z) \\ F_3(z) \end{bmatrix} e^{i\omega[t - (m/c)x]}; \quad (6)$$

m is a constant and will be determined later. If we introduce new symbols $\lambda_p = \lambda/p\sqrt{\epsilon}$ and $\bar{m} = m/\sqrt{\epsilon}$, we obtain from Eqs. (5) and (6)

$$F_3 - i\lambda_p \frac{\bar{m}}{m^2 - \epsilon_3/\epsilon} \frac{dF_1}{d\alpha} = 0 \quad (7)$$

and

$$\frac{d^2 F_1}{d\alpha^2} + (\bar{a}_1 + \bar{a}_2 \cos 2\alpha) F_1 + \bar{a}_2 \sin 2\alpha F_2 = 0, \quad (8a)$$

$$\frac{d^2 F_2}{d\alpha^2} + (\bar{b}_1 - \bar{b}_2 \cos 2\alpha) F_2 + \bar{b}_2 \sin 2\alpha F_1 = 0. \quad (8b)$$

$\alpha = 2\pi z/p$, and $\bar{a}_1, \bar{a}_2, \bar{b}_1,$ and \bar{b}_2 are constants, determined by the structure parameters $\epsilon, \epsilon_3, \beta$, and p and the experimental conditions given by the frequency ω and the parameter m , which is essentially determined by the angle of incidence, as will be shown later:

$$\begin{aligned} \bar{a}_1 &= \epsilon \left(\frac{p}{\lambda}\right)^2 \left(1 - \frac{m^2}{\epsilon_3}\right), \\ \bar{a}_2 &= \left(\frac{p}{\lambda}\right)^2 \frac{\epsilon_1 - \epsilon_2}{2} \left(1 - \frac{m^2}{\epsilon_3}\right), \\ \bar{b}_1 &= \left(\frac{p}{\lambda}\right)^2 (\epsilon - m^2), \\ \bar{b}_2 &= \left(\frac{p}{\lambda}\right)^2 \frac{(\epsilon_1 - \epsilon_2)}{2}. \end{aligned} \quad (9)$$

For the case that the waves do not propagate in the xz plane of the twisted structure but in a plane that is rotated by an angle ϕ around the z axis, we have

$$\begin{bmatrix} E_x \\ E_y \\ E_z \end{bmatrix} = \begin{bmatrix} f_1(z) \\ f_2(z) \\ f_3(z) \end{bmatrix} \times \exp \left[i\omega \left(t - \frac{m}{c} (x \cos \phi + y \sin \phi) \right) \right], \quad (10)$$

and we again get the system (8) of differential equations.

As we will see later, this is the reason why the reflection bands of the twisted structure depend only on the angle of incidence and not on the azimuthal directions. The azimuthal angle influences the intensity of the wave but not the position of the

reflection bands.

The system (7) of differential equations is equiv-

alent to an ordinary fourth-order differential equation:

$$\begin{aligned} \varphi^{(4)} + 4 \frac{\cos 2\alpha}{\sin 2\alpha} \varphi^{(3)} + \left[4 + 8 \frac{\cos 2\alpha}{\sin 2\alpha} + A_1 + A_2 \cos 2\alpha + B_1 - B_2 \cos 2\alpha \right] \varphi'' + \left[-4A_1 \frac{\cos 2\alpha}{\sin 2\alpha} - 4 \frac{A_2}{\sin 2\alpha} \right] \varphi' \\ + \left[4A_1 + 8(A_1 + A_2) \frac{\cos 2\alpha}{\sin 2\alpha} + (A_1 + A_2 \cos 2\alpha)(B_1 - B_2 \cos 2\alpha) - A_2 B_2 \sin^2 2\alpha \right] \varphi = 0, \end{aligned} \quad (11)$$

with constants A_1 , A_2 , B_1 , and B_2 .

We can obtain a simpler equation by assuming the medium to be locally uniaxial. This means that in the local coordinate system (ξ, η, ζ) two of the three dielectric constants will be equal. Therefore in the following calculations we assume

$$\epsilon_2 = \epsilon_3. \quad (12)$$

If φ and χ , given by

$$\varphi = F_1 \cos \alpha + F_2 \sin \alpha, \quad (13)$$

$$\chi = -F_1 \sin \alpha + F_2 \cos \alpha,$$

are the components of the vector \vec{F} in the twisted system, then instead of (8) we obtain the equations

$$\frac{d^2 \varphi}{d\alpha^2} - 2 \frac{d\chi}{d\alpha} + a_1 \varphi + a_2 \varphi \cos 2\alpha = 0, \quad (14)$$

$$\frac{d^2 \chi}{d\alpha^2} + 2 \frac{d\varphi}{d\alpha} + b_1 \chi - a_2 \varphi \sin 2\alpha = 0,$$

or the equivalent fourth-order equation:

$$\begin{aligned} \frac{d^4 \varphi}{d\alpha^4} + (a + a_2 \cos 2\alpha) \frac{d^2 \varphi}{d\alpha^2} - (6a_2 \sin 2\alpha) \frac{d\varphi}{d\alpha} \\ + (b + da_2 \cos 2\alpha) \varphi = 0, \end{aligned} \quad (15)$$

where

$$a = 4 + a_1 + b_1, \quad b = a_1 b_1, \quad d = b_1 - 8, \quad (15a)$$

and

$$\begin{aligned} a_1 &= \frac{1}{\lambda_p^2} \left[1 + \beta - 0.5 \bar{m}^2 \left(\frac{\epsilon(1+\beta)}{\epsilon_3} + 1 \right) \right] - 1, \\ b_1 &= \frac{1}{\lambda_p^2} \left[1 - \beta - 0.5 \bar{m}^2 \left(\frac{\epsilon(1-\beta)}{\epsilon_3} + 1 \right) \right] - 1, \\ a_2 &= -\frac{1}{\lambda_p^2} \frac{1}{2} \bar{m}^2 \left(\frac{\epsilon(1-\beta)}{\epsilon_3} - 1 \right), \\ b_2 &= \frac{1}{\lambda_p^2} \frac{1}{2} \bar{m}^2 \left(\frac{\epsilon(1-\beta)}{\epsilon_3} - 1 \right). \end{aligned} \quad (15b)$$

The system of equations (14) is identical with expressions given by Oseen.²

Equation (14) is a system of second-order linear homogeneous differential equations with periodic coefficients. According to Floquet's theorem⁶ there exists at least one solution $\varphi(\alpha)$ which obeys

the functional equation

$$\varphi(\alpha + \pi) = \sigma \varphi(\alpha) = e^{i\pi\mu} \varphi(\alpha), \quad (16)$$

where σ is an appropriate constant $\sigma = e^{i\pi\mu}$. Moreover, there exists in general a system of linearly independent solutions of the form

$$\varphi_j(\alpha) = e^{i\mu_j \alpha} P_j(\alpha), \quad j = 1, 2, 3, 4 \quad (17)$$

where the $P_j(\alpha)$ are periodic functions with period π :

$$P_j(\alpha + \pi) = P_j(\alpha). \quad (18)$$

To show this, we assume a fundamental system of solutions φ_j ,

$$\varphi_j = y_j(\alpha), \quad j = 1, 2, 3, 4, \quad (19)$$

of the differential equation (15) which satisfy the initial conditions

$$\frac{d^n y_j(\alpha_0)}{d\alpha^n} = \delta_{j, n+1}; \quad j = 1, 2, 3, 4, \quad n = 0, 1, 2, 3, \quad 0 \leq \alpha_0 \leq \pi. \quad (20)$$

The $\delta_{i, n}$ are the Kronecker symbols.

Since the coefficients of the differential equation have the period π , this means that if $y_j(\alpha)$ is a solution, then $y_j(\alpha + \pi)$ is also a solution, which can be represented by the constants $a_{i, j}$ in the following way:

$$y_n(\alpha + \pi) = \sum_{j=1}^4 a_{n, j} y_j(\alpha). \quad (21)$$

Similar equations hold for the first, second, and third derivatives of the functions $y_n(\alpha)$. From this system of equations and the initial conditions (20) we obtain for $\alpha_0 = 0$ the relations

$$\frac{\partial^l y_n(\pi)}{\partial \alpha^l} = a_{n, l+1}; \quad n = 1, 2, 3, 4, \quad l = 0, 1, 2, 3. \quad (22)$$

If there exists a solution with the property (16), it must then be possible to describe it in terms of constants H_i ($i = 1, 2, 3, 4$) by

$$\varphi(\alpha) = \sum_{i=1}^4 H_i y_i(\alpha). \quad (23)$$

The y_i are linearly independent because of the different initial conditions. From (16) and (21) we get

$$\sum_{n=1}^4 (a_{jn} - \sigma \delta_{jn}) H_n = 0, \quad j=1, 2, 3, 4.$$

There exists a nontrivial solution only when the determinant of coefficients vanishes:

$$\begin{vmatrix} a_{11} - \sigma & a_{12} & a_{13} & a_{14} \\ a_{21} & a_{22} - \sigma & a_{23} & a_{24} \\ a_{31} & a_{32} & a_{33} - \sigma & a_{34} \\ a_{41} & a_{42} & a_{43} & a_{44} - \sigma \end{vmatrix} = 0. \quad (24)$$

This is the characteristic equation for the differential equation (15). In general, there will be four different solutions $\sigma_j = e^{i\pi\mu_j}$ and, correspondingly, four linearly independent solutions $\varphi_j(\alpha)$ which satisfy Eqs. (16). From this it immediately follows that the P_i in (17) are periodic with a period π :

$$P_j(\alpha) = e^{-\mu_j \alpha} \varphi_j(\alpha). \quad (25)$$

The characteristic equation (24) can be put into a simpler form. The symmetry of the differential equation (15) is such that if μ is a characteristic exponent, $-\mu$ is also a characteristic exponent. Therefore Eq. (24) has the form

$$\sigma^4 + a\sigma^3 + b\sigma^2 + a\sigma + 1 = 0, \quad (26)$$

where the constants a and b are given by the real quantities a_{ij} of Eq. (24). The solutions $\sigma_j = e^{i\pi\mu_j}$, $j=1-4$, of Eq. (26) can be given in closed form.

It is possible to make a further simplification by combining two solutions which have the same absolute value of the characteristic exponents to obtain $\cos\pi\mu$. Equation (26) becomes a quadratic equation in $\cos\pi\mu$ with real coefficients. This equation does not determine the characteristic exponents μ uniquely, but only gives them modulo some integer:

$$\mu = \mu_0 + n, \quad n=0, \pm 1, \pm 2, \dots$$

We have shown above that $P(\alpha)$ (we omit the subscript in the following treatment) is periodic and therefore this function can be expanded in a Fourier series:

$$P(\alpha) = \sum_{n=-\infty}^{\infty} c_n e^{2in\alpha}. \quad (27)$$

Likewise $\varphi(\alpha)$ is given by the series

$$\varphi(\alpha) = \sum_{n=-\infty}^{\infty} c_n e^{i(2n+\mu)\alpha} \quad (28)$$

and with the same characteristic exponent,

$$\chi(\alpha) = \sum_{n=-\infty}^{\infty} d_n e^{i(2n+\mu)\alpha}. \quad (29)$$

Inserting into Eqs. (14) we obtain the following recursion relationships for the coefficients c_n and d_n :

$$d_k = D_k c_k + F_k (c_{k-1} + c_{k+1}), \quad (30)$$

$$\alpha_k c_k + \beta_{k-1} c_{k-1} + \gamma_k c_{k+1} = 0, \quad (31)$$

$$k=0, \pm 1, \pm 2, \dots$$

Here we have introduced the following notations:

$$\alpha_k = (2k + \mu)^4 - a(2k + \mu)^2 + b,$$

$$\beta_k = \frac{1}{2} a_2 [d - 6(2k + \mu) - (2k + \mu)^2],$$

$$\gamma_k = \frac{1}{2} a_2 [d + 6(2k + \mu) - (2k + \mu)^2], \quad (32)$$

$$D_k = \frac{2i(2k + \mu)}{b_1 - (2k + \mu)},$$

$$F_k = \frac{a_2}{2i} \frac{1}{b_1 - (2k + \mu)}.$$

a , b , d , b_1 , and a_2 are given by Eq. (15). If one coefficient, say c_0 , is fixed all the other c_n and also the d_n are completely determined.

Now we can evaluate the electric field from Eqs. (7) and (13). For each of the partial waves belonging to one of the four different characteristic exponents, we obtain a solution of the form

$$\begin{bmatrix} E_x \\ E_y \\ E_z \end{bmatrix} = \begin{bmatrix} \bar{f}_1(z) \\ \bar{f}_2(z) \\ \bar{f}_3(z) \end{bmatrix} \exp \left[i\omega \left(t - \frac{m}{c} x + \frac{\mu}{c} \frac{\lambda}{p} z \right) \right] \quad (33)$$

The functions $\bar{f}_1(z)$, $\bar{f}_2(z)$, and $\bar{f}_3(z)$ are periodic with period p :

$$\bar{f}_j(z+p) = \bar{f}_j(z). \quad (34)$$

They still have twice the period of the structure even though we have assumed a nonpolar ordering so that the structure repeats itself after a twist angle of $\alpha = \pi$. λ is the wavelength in vacuum and ω the frequency. μ and m are constants; μ is determined by the structure parameters ϵ_1 , ϵ_2 , and p and also by the constant m , as will be shown later. For fixed parameters there will exist four characteristic exponents μ which can be grouped into two conjugate pairs of opposite sign.

It can be shown that the boundary conditions at the isotropic to twisted dielectric interface can be fulfilled by the two waves whose characteristic exponents have different absolute values. We are therefore able to completely describe the light transmission and reflection properties of a uniformly twisted dielectric.

PROPERTIES OF THE NORMAL WAVES

Equation (33) shows that wave propagation in a twisted dielectric differs from that in an ordinary anisotropic medium. Depending on whether the characteristic exponent μ is real or complex, the corresponding normal wave (33) can propagate (stable wave) or is damped (unstable wave). This

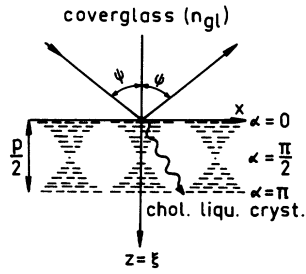


FIG. 2. Sample geometry. The boundary of the liquid crystal is assumed to be normal to the helical axis. The plane of incidence is the xz plane.

are obtained from Eq. (39). The reason is that we have lost the periodicity in μ of the determinant by truncating it. In practice a series of integers has therefore to be inserted. An exact closed expression for the starting points of the characteristic curves is derived below (Eq. 42) which helps to decide which integer number has to be taken to get a desired curve. For computer calculations another form of the characteristic equation (39) may be useful. The infinite determinant is equivalent to a chain fraction. Therefore if we confine again to the truncated form we get, instead of Eq. (39),

$$\frac{g_0}{1 - \frac{g_{-1}}{1 - \frac{g_{-2}}{1 - \frac{g_{-3}}{\ddots}}}}} + \frac{g_1}{1 - \frac{g_2}{1 - \frac{g_3}{1 - \frac{g_4}{\ddots}}}} = 1 \quad (39')$$

The g_k are given by

$$g_k = \frac{\gamma_k \beta_{k-1}}{\alpha_k \alpha_{k-1}}.$$

α_k , β_k , and γ_k are taken from Eq. (32).

CHART OF STABILITY

The characteristic exponent μ is determined by the material parameters ϵ , β , and p and by the reduced wavelength λ_p and the angle of incidence ψ , which is related to \bar{m} . For a given material ϵ , β , and p are fixed and the stability is determined by λ_p and \bar{m} only. We have shown that the boundaries between regions of stability and instability are characterized by integer characteristic exponents. In a λ_p, \bar{m} diagram, therefore, the characteristic curves

$$\mu(\lambda_p, \bar{m}) = n, \quad n = 0, \pm 1, \pm 2, \dots \quad (40a)$$

or

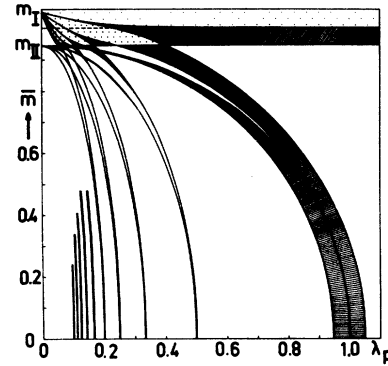


FIG. 3. Chart of stability. The periodic structure of cholesteric liquid crystals gives rise to "forbidden bands" (regions of instability; shaded regions in the figure). One of the normal waves is not allowed to propagate for given frequency and wave vector. For the dotted regions both normal waves are forbidden to propagate. $\bar{m} = (n_{gl} / \sqrt{\epsilon}) \sin \psi$ gives the direction of the incident wave and defines the wave vector of the normal waves in the liquid crystal; n_{gl} , refractive index of the boundary isotropic medium; λ_p is the reduced wavelength, $\lambda_p = \lambda / p\sqrt{\epsilon}$, where p is the pitch of the helicoidal structure. The figure was computed for $\epsilon = 2.27$, $\epsilon_1 - \epsilon_2 = 0.48$.

$$G_\mu(\lambda_p, \bar{m}) = 0, \quad \mu = 0, \pm 1, \pm 2, \dots \quad (40b)$$

separate regions of stable waves from those of unstable solutions: We get a chart of stability. Such a chart is shown in Fig. 3 for $\epsilon = 2.27$, $\delta = \epsilon_1 - \epsilon_2 = 0.48$, respectively $\beta = 0.1057$. These parameters are assumed to be independent of wavelength. The shaded and dotted regions indicate the regions where the solutions are unstable. For all other parameters the waves are stable.

A wave incident to a twisted structure will, in general, excite two normal waves which are usually transmitted. However, if the wavelength falls into a "forbidden" region (region of instability) the wave will be damped out, and since we neglect absorption, it will be totally reflected. For parameters in the shaded regions, only one normal wave is reflected, the other being transmitted. In the dotted region both waves will be totally reflected. Figure 4 shows the situation for

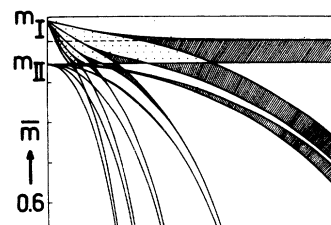


FIG. 4. Enlarged segment of the chart of stability given in Fig. 3.

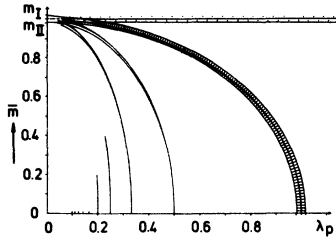


FIG. 5. Chart of stability for a cholesteric liquid crystal having $\epsilon = 2.27$, $\epsilon_1 - \epsilon_2 = 0.16$.

$\bar{m} \sim 1$ where the characteristic curves pile up. We see that each region of reflection consists of two noncrossing parts. The long-wavelength branches end on the \bar{m} axis at the point \bar{m}_I , whereas the short-wavelength branches end at \bar{m}_{II} . Each short-wavelength branch is crossed by the long-wavelength branches of all the reflection bands of high-order.

The chart of stability of Fig. 3 shows a series of curves that can be divided into two groups. Those of the one group are infinite in number and all depart from the abscissa and end in one of the two points, $m_I = (\epsilon_1/\epsilon)^{1/2}$ and $m_{II} = (\epsilon_2/\epsilon)^{1/2}$ on the ordinate (see also Fig. 5 and Fig. 6). We have only indicated those for the longer wavelengths. These curves separate the regions of selective reflection, caused by the helical structure, from those of transmittance. In other words, they border bandpasses or bandstops. The other group consists of only two curves. For very large λ_p they are parallel to the λ_p axis. These curves give the ordinary total reflection for light passing from an optically dense to a less dense medium. One of these two curves is the straight line $\bar{m} = (\epsilon_2/\epsilon)^{1/2}$. Using Eq. (36) we see that it corresponds to a critical angle ψ_c given by

$$n_{gl} \sin \psi_c = \sqrt{\epsilon_2}. \quad (41a)$$

The corresponding wave travels perpendicular to the helical axis with the dielectric vector parallel to the z axis. This can easily be verified by introducing $\bar{m} = \epsilon_2/\epsilon$ into Eqs. (7) and (8). The other boundary curve of total reflection is dependent on λ_p . It starts at $\bar{m} = (\epsilon_1/\epsilon)^{1/2}$, $\lambda_p = 0$, corresponding to a critical angle ψ_c given by

$$n_{gl} \sin \psi_c = \sqrt{\epsilon_1}, \quad (41b)$$

and decreases rapidly with increasing λ_p to $\bar{m} = 1$, corresponding to a critical angle given by

$$n_{gl} \sin \psi_c = \sqrt{\epsilon}. \quad (41c)$$

In the limiting case $\lambda_p \rightarrow 0$ the critical angles of total reflection are related to ϵ_2 and ϵ_1 , respectively [see Eqs. (41a) and (41b)]. If the pitch is

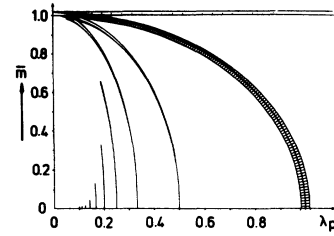


FIG. 6. Chart of stability for a cholesteric liquid crystal with oblate local dielectric tensor ellipsoid; $\epsilon = 2.27$, $\epsilon_1 - \epsilon_2 = -0.16$.

comparable or small compared to the wavelength, the angles of total reflection are determined by the dielectric constants ϵ_2 and ϵ [see Eqs. (41a) and (41c)]. This result is important for measurements of the refractive indices of cholesteric liquid crystals by total reflection.

From Eq. (39) we see that the starting points $\lambda_p^{(k)}$ of the first group of curves on the λ_p axis ($m = 0$) are given by the simple equation

$$\lambda_p^{(k)} = \frac{(\epsilon_1 \epsilon_2)^{1/2}}{\left\{ \epsilon^2 (1 + k^2) \pm \epsilon \left[\epsilon^2 (1 + k^2)^2 - (k^2 - 1)^2 \epsilon_1 \epsilon_2 \right]^{1/2} \right\}^{1/2}} \quad (k = 0, 1, 2, \dots). \quad (42)$$

For $k = 0$ we get the boundaries of the region of reflection (in agreement with de Vries):

$$\lambda_{pI}^{(0)} = (\epsilon_1/\epsilon)^{1/2}, \quad \lambda_{pII}^{(0)} = (\epsilon_2/\epsilon)^{1/2}. \quad (43)$$

For oblique incidence we find additional regions of reflection which are not given by the de Vries theory. Eq. (42) shows that the other points $\lambda_p^{(k)}$ ($k \neq 0$) pile up at $\lambda_p = 0$. For very large k Eq. (42) approximately gives

$$\lambda_p^{(k)} \approx 1/k \quad (k = \text{integer}). \quad (44)$$

This relation indicates that the additional reflection bands correspond to higher-order harmonics.

In contrast to (44), which gives only one value of λ_p for each k , the exact relation (42), however, gives two neighboring points, except for the case of the main reflection band. This is shown in Table I, where the $\lambda_p^{(k)}$ values are given for $k = 0$ up to $k = 9$ ($\epsilon = 2.27$, $\delta = 0.16$ or $\beta = 0.03524$).

As pointed out by Oseen² and later by de Vries³ there exists only one reflection band for $\bar{m} = 0$ (normal incidence). This is the region between λ_{pI} and λ_{pII} . For all the other points of the λ_p axis ($m = 0$) the waves are stable and no reflection occurs. The higher-order reflection bands have vanishing width at normal incidence. This is a special feature of helical structures.

Another chart of stability is given by Fig. 5. For computation we used the same dielectric con-

TABLE I. Intercepts $\lambda_p^{(k)}$ of the boundary curves of the first nine reflection bands at the λ_p axis for $\epsilon_1 = 2.35$ and $\epsilon_2 = 2.19$. $k = 0$ gives the wavelength limits of the main reflection band for normal incidence. For $k = 2$ the value about 1 represents the point at the λ_p axis from which the splitting of the main band for oblique incidence originates. All other $\lambda_p^{(k)}$ values correspond to the intersections of the two boundary curves which border one branch of the higher reflection bands.

k	$\lambda_p^{(k)}$	k	$\lambda_p^{(k)}$
0	0.982221 1.017468	5	0.166481 0.250124
1	0.499689	6	0.142676 0.200129
2	0.333100 1.000077	7	0.124823 0.166799
3	0.249793 0.500103	8	0.110937 0.142992
4	0.199806 0.333449	9	0.099828 0.125137

stant as before ($\epsilon = 2.27$) but the dielectric anisotropy being one-third of the preceding example ($\delta = 0.16$; $\beta = 0.03524$). As a consequence the reflection bands are much narrower than before.

For the examples shown in Figs. 3 and 5 we assumed $\epsilon_1 > \epsilon_2$ ($\beta > 0$). If $\epsilon_1 < \epsilon_2$ ($\beta < 0$) a different stability chart results because Eq. (15) is not symmetrical in ϵ_1 and ϵ_2 . Figure 6 shows such a diagram for $\epsilon = 2.27$, $\beta = -0.03524$ with the same β as in Fig. 5 but of opposite sign (negative dielectric anisotropy). The broad and the narrow branches of the regions of reflection have changed their positions: For a prolate dielectric ellipsoid, the narrow branch is on the short-wavelength side and for an oblate ellipsoid it is at the long-wavelength side. Therefore a measurement of the reflectivity at larger angles of incidence gives directly the relative values of the dielectric constants (the absolute values could be evaluated from the normal incidence).

ANALOGY BETWEEN CHOLESTERIC SELECTIVE REFLECTION AND BRAGG REFLECTION

Selective reflection has been compared to Bragg reflection (see Ref. 1) and we have supported this analogy by giving the approximate equation (44):

$$\lambda_k = (1/k)\lambda_0 \quad (\lambda_0 = p\sqrt{\epsilon}, \quad k = 1, 2, 3, 4, \dots)$$

for the center of the reflection bands at nearly normal incidence. It shall be emphasized, however, that for normal incidence (propagation parallel to the helical axis) only one reflection band exists. According to Bragg's law for oblique incidence the wavelength λ of the reflected light and the angle of incidence ψ are connected by

$$\lambda = p(\epsilon - n_{gl}^2 \sin^2 \psi)^{1/2}. \quad (45)$$

Here it is assumed that light is incident from an isotropic medium with refractive index n_{gl} onto a system of reflection planes with the distance $\frac{1}{2}p$ and which are embedded in a dielectric with dielectric constant ϵ .⁷ An analogous relationship can be derived in our formalism. It can be easily shown that Eq. (39) is satisfied by $b_1 = 0$, i.e.,

$$\lambda = p(\epsilon_2 - n_{gl}^2 \sin^2 \psi)^{1/2}. \quad (46)$$

This relation holds exactly and not only in the approximation of Eq. (39).

In a chart of stability Eq. (46) gives one of the characteristic curves: It limits the first-order reflection band on the short-wavelength side if $\epsilon_1 > \epsilon_2$. For higher-order reflection bands this analytic expression can no longer be applied. The simple Bragg reflection formula, therefore, only holds at one of the boundaries of the first-order reflection band.

ACKNOWLEDGMENT

We wish to express our gratitude to A. Saupe for bringing this problem to our attention and for many stimulating discussions.

¹J. L. Fergason, *Mol. Cryst. Liq. Cryst.* **1**, 293 (1966).

²C. W. Oseen, *Ark. Mat. Astron. Fys.* **21A**, 14 (1928); *Ark. Mat. Astron. Fys.* **21A**, 1 (1929); *Trans. Faraday Soc.* **29**, 883 (1933).

³H. de Vries, *Acta Crystallogr.* **4**, 219 (1951).

⁴D. W. Berreman and T. J. Scheffler, *Mol. Cryst. Liq. Cryst.* **11**, 395 (1970); *Phys. Rev. Lett.* **25**, 577 (1970).

⁵D. Taupin, *J. Phys. (Paris)* **30**, C4-32 (1969).

⁶See, e.g., L. Cesari, *Asymptotic Behaviour and Stability Problems in Ordinary Differential Equations* (Springer, Berlin, 1959).

⁷Fergason derived the formula $\lambda = \lambda_n(\cos \frac{1}{2} \{\sin^{-1}[(1/1.5)\sin\psi_I] + \sin^{-1}[(1/1.5)\sin\psi_S]\})$, where ψ_I and ψ_S are the angles of incidence and observation, respectively. For a uniformly oriented helical structure (planar structure) $\psi_I = \psi_S = \psi$ and this equation reduces to (45).